

# Optical thickness monitoring sensitivity improvement using graphical methods

Ronald R. Willey

Semidirect level monitoring has error compensation capabilities of potential benefit to optical coatings of certain types. A review of the principles of level monitoring using circle diagrams shows how to design a level monitoring scheme for various cases, including the use of precoated monitoring chips. The film thickness sensitivities for various optical monitoring strategies differ considerably. Optimum level trigger point monitoring offers improved sensitivity of change in reflectance vs change in optical thickness. This procedure is also expected to give small thickness errors when optically monitored. Optimum level trigger point monitoring, and its application, is fully described.

## I. Introduction

This paper describes optical monitoring strategies expected to improve precision and repeatability of the optical thickness of thin film coatings. Macleod and Pelletier<sup>1</sup> reviewed level monitoring, and Zhao<sup>2</sup> elaborated on its application. Compensation effects can give good results at the monitoring wavelength, but the magnitude of errors in measuring optical thickness causes performance to deteriorate at wavelengths other than the monitoring wavelength.

We believe better optical thickness sensitivity is the key factor in obtaining better precision and repeatability at wavelengths other than the monitoring wavelength. This is predicated on the belief that optical monitoring better controls optical thickness than does deposited mass monitoring (crystal monitoring). However, the latter frequently does have a number of advantages. Macleod<sup>3</sup> and Thoni<sup>4</sup> have pointed out that the index of refraction may be more important in some classes of coating than the optical thickness. Vidal and Pelletier<sup>5</sup> have shown the potential of broadband monitoring techniques in dealing with many of these effects. Schroedter<sup>6</sup> has presented a useful method which combines data of the optical and crystal monitors in real time.

This report deals only with the simplest case of using a single-wavelength monitor to control optical thick-

ness and the crystal to control the rate of deposition. The conditions which we studied can be directly implemented on standard commercially available systems such as described by Willey.<sup>7</sup> It appears that an order of magnitude improvement in repeatability of coating performance over turning point monitoring may be possible with our strategies.

## II. Principles of Semidirect Level Monitoring

Our work deals exclusively with semidirect monitoring. The latter is defined as applying every deposited layer onto the monitor chip. Direct monitoring is defined as monitoring the reflectance or transmittance of the actual part to be coated throughout the depositions. Indirect monitoring is defined as using two or more monitor chips for different layers of the coating being applied. In the latter case, succeeding layers cannot generally compensate for errors in the previous layer.

Semidirect monitoring has the advantage over direct monitoring in that a precoat, not on the part being coated, can be applied to the monitor chip. However, it has the disadvantage that angular distribution of the sources, and temperature effects, may cause nonproportionality in the amount of material reaching the monitor chip vs the part being coated. Yet, if this effect is reproducible from run to run, corrections can be made for it.

Macleod, Pelletier, and Zhao have shown that error compensation effects are possible with proper monitoring strategies. The latter are similar to those found in direct monitoring of the passband in narrow passband (Fabry-Perot) filters. Zhao shows furthermore that error effects are minimized at the monitoring wavelength and increase with distance from the monitoring wavelength. These off-wavelength errors are a

The author is with Opto Mechanik, Inc., P.O. Box 640, Melbourne, Florida 32902-0640.

Received 20 October 1986.

0003-6935/86/040729-09\$02.00/0.

© 1986 Optical Society of America.

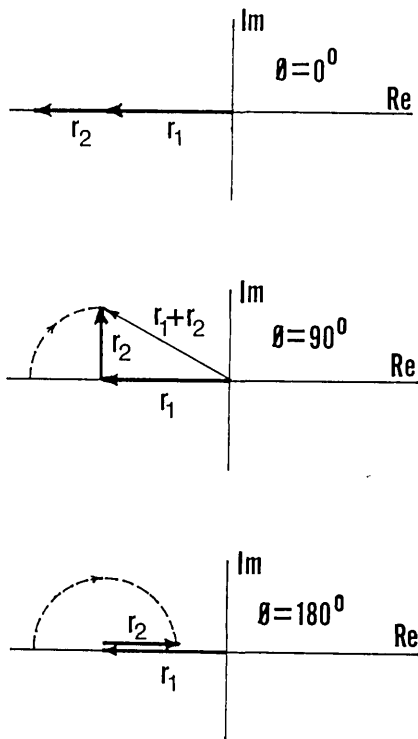


Fig. 1. Addition of amplitude vectors of reflections from the two surfaces of a thin film for various phase angles (thicknesses).

function of the magnitude of the errors which exist but are compensated at the monitoring wavelength. If we can improve accuracy at the monitoring wavelength, the broadband result should also benefit.

### III. Reflectance Diagrams

Apfel<sup>8</sup> elaborated on the use of circle diagrams or reflectance amplitude diagrams in optical coating design. A brief review of the basic concepts will help illustrate the monitoring design strategies described in this paper.

Reflectance amplitude at a single interface of two dielectric materials of indices of refraction  $n_1$  and  $n_2$  is defined as  $r$ , where  $r = (n_1 - n_2)/(n_1 + n_2)$ .

The intensity of radiation reflected at an interface is given by  $R = rr^*$ .

In measuring a thin film on a substrate,  $r_1$  is the first surface reflection,  $r_2$  is the second, the phase thickness of the film is  $\varphi$ , and the reflectance amplitude resulting from the two surfaces is  $r = [r_1 + r_2 \exp(-i\varphi)]/[1 + r_1 r_2 \exp(-i\varphi)]$ .

Figure 1 illustrates the equations in the approximate vector form and indicates qualitatively how the circles arise. The remainder of the figures are calculated using the complete expression. Figure 2 shows the typical quarterwave optical thickness (QWOT) of magnesium fluoride on crown glass. Note the small reflectance change (4.3–1.2%) at the lowest reflectance wavelength. Figure 3 shows the reflectance spectrum, and Fig. 4 demonstrates the optical monitor signal change as film thickness increases. Again note the small change in reflectance.

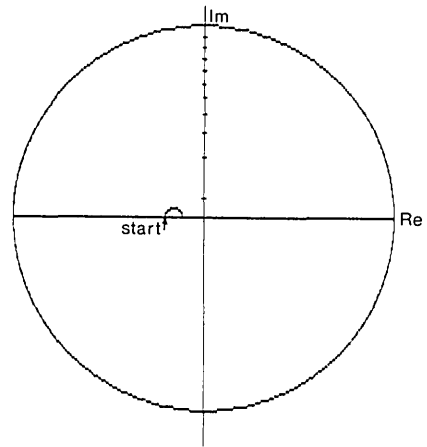


Fig. 2. Reflectance amplitude diagram for a quarterwave optical thickness of magnesium fluoride on a crown glass substrate.

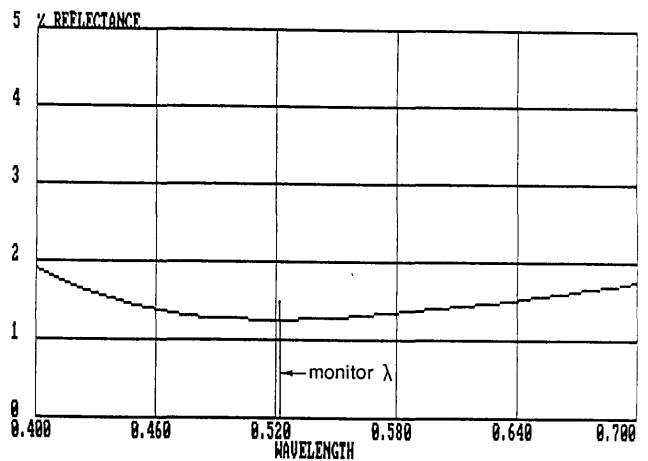


Fig. 3. Reflectance spectrum of a QWOT of magnesium fluoride on a crown glass substrate.

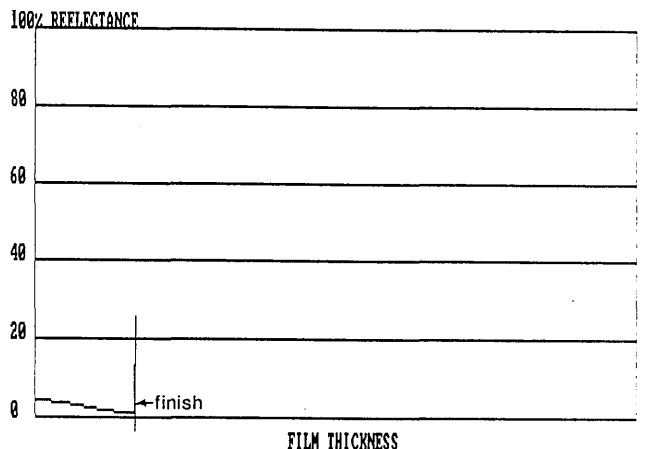


Fig. 4. Optical monitor signal change as the film thickness increases during deposition of a QWOT of magnesium fluoride on a glass substrate.

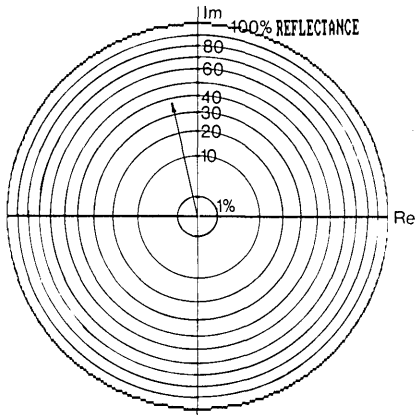


Fig. 5. Reflectance diagram of equal percent reflectance intensity contours. The vector represents a reflectance intensity of  $\sim 36\%$  and a reflectance amplitude of 0.60.

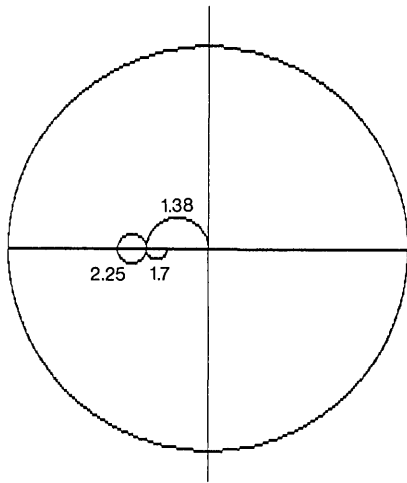


Fig. 6. Circle diagram for a classical quarter-half-quarterwave broadband antireflection coating at the design wavelength.

Figure 5 illustrates equal intensity contours on the reflectance diagram. The vector represents a reflectance intensity of  $\sim 36\%$  and a reflectance amplitude of 0.60. Equal amplitude contours would be in equal increments of radius from 0.0 at the origin to 1.0 at the circumference.

Admittance diagrams as described by Macleod<sup>9</sup> show a very similar appearance except for a conformal mapping. They serve the same general function as reflectance diagrams and possess certain advantages and disadvantages depending on the application and personal preference.

Figure 6 illustrates the circle diagram for a classical quarter-half-quarterwave broadband antireflection coating. Figure 7 depicts the spectral reflectance curve, and Fig. 8 shows what the optical monitor signal would look like on a single-monitor chip (semidirect monitoring). The layer terminations are made at turning points, and although the gamut is better than the single-layer magnesium fluoride, it is still low.

Figure 9 is a circle diagram for a QWOT stack of HLHLHLHL on crown glass. At the QWOT wave-

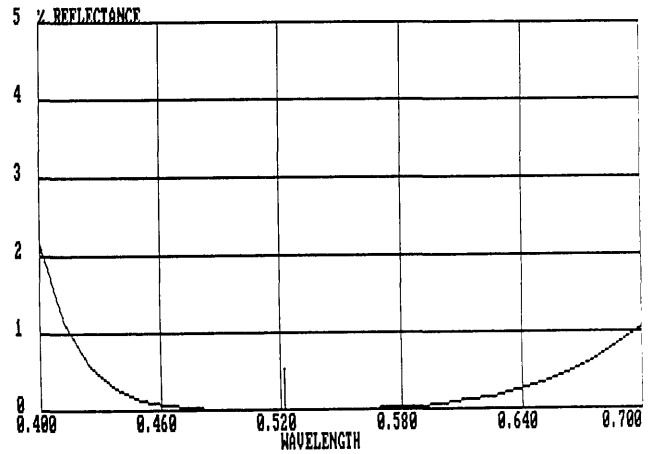


Fig. 7. Spectral reflectance curve for a quarter-half-quarter antireflection coating showing the design wavelength at  $0.520 \mu\text{m}$ .

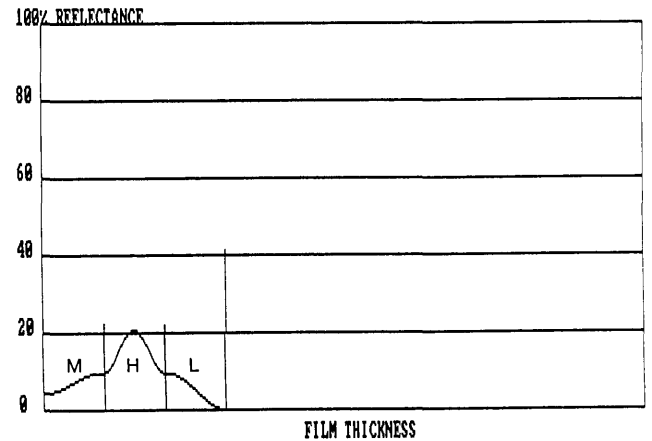


Fig. 8. Optical monitor signal on a single-monitor chip (semidirect monitoring) for the classic quarter-half-quarter antireflection coating.

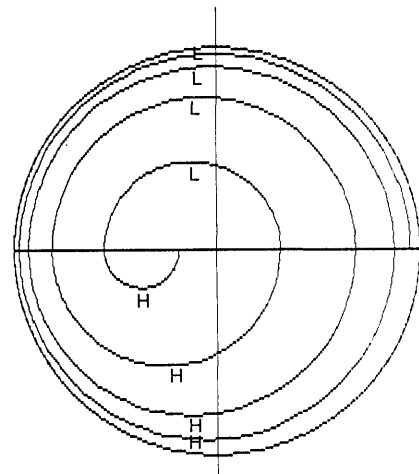


Fig. 9. Circle diagram for a QWOT stack of HLHLHLHL on crown glass. At the QWOT wavelength, the reflectance increases with each layer.

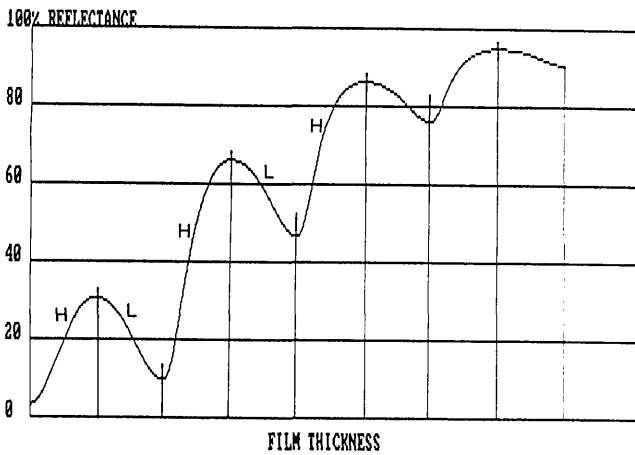


Fig. 10. Optical monitor curve of the QWOT stack HLHLHLHL on crown glass.

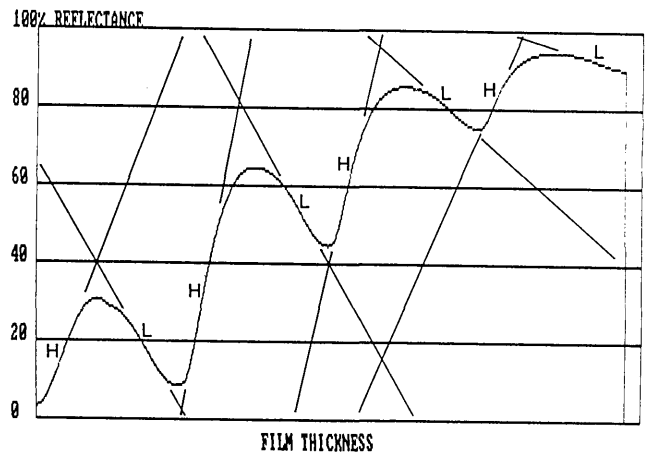


Fig. 11. Optical monitor curve of the HLHLHLHL QWOT stack to show: the relatively flat spots, that the maximum slopes of the curves are greater for the high-index than the low-index layers, and that the slopes are greatest for layers whose reflectance is in the 20-60% intensity range and diminishes as the reflectance becomes greater or less than this level.

length the reflectance increases with each layer. Figure 10, the monitor curve, illustrates this.

These graphic forms are basic for our demonstration that the sensitivity of reflectance changes with optical thickness. Finally, being able to choose more sensitive monitoring strategies for various types of coating is a major result of our work.

#### IV. Sensitivity

Macleod and Pelletier<sup>1</sup> illustrated the relative insensitivity of turning point monitoring to optical film thickness. The rate of change of reflectance with film thickness goes to zero at the turning points making it difficult to pick the latter precisely, particularly in the presence of any noise in the signal. They also point out that skilled operators do better than might be expected by using small but consistent overshoots of the turning points to get to a point where the rate of change is observable.

Figure 11 is again the HLHLHLHL QWOT stack used to point out relatively flat spots at turning points where large errors in thickness cause only small changes in reflectance. This figure also shows three other key points for discussion.

(1) The rate of change of reflectance with thickness is seen to be greatest midway between the turning points. The greatest potential precision in film thickness control can be obtained by performing the cutoff at these levels.

(2) The maximum slopes of the curves are greater for the high-index than the low-index layers.

(3) The slopes are greatest for layers whose reflectance is in the 20-60% intensity range and diminishes as the reflectance moves outside this level.

We developed a computer program to analyze the rate of change of reflectance vs optical film thickness for any desired index layer being deposited on a complete range of substrate admittances. This analysis is illustrated in Fig. 12 and is the key point of this paper.

Although Fig. 12 is for a magnesium fluoride layer, we found that the curves are almost identical for most other indices. Note that the magnitude of sensitivity

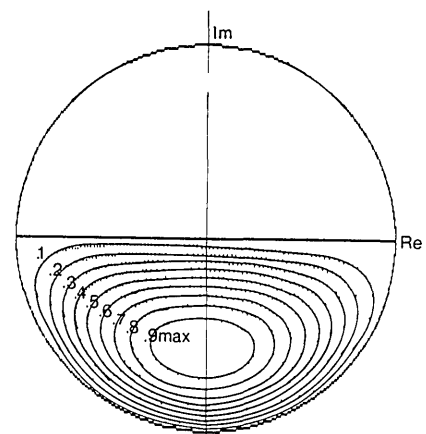


Fig. 12. Rate of change of reflectance intensity with optical film thickness material of index 1.38 as a function of position on the reflectance circle diagram. Values are symmetric about the real axis.

is approximately proportional to the index of refraction minus one ( $n - 1$ ). The sensitivity goes to zero on the real axis and has its maximum near a reflectance amplitude of 0.6 (or reflectance intensity of 36%) on the imaginary axis. This is consistent with Fig. 11. The visualization provided by Fig. 12 helps us to better understand the results reported by Macleod and others which we use as illustrations in the next section.

#### V. Examples of Sensitivity

Macleod and Pelletier<sup>1</sup> analyzed the results obtained by Ward<sup>10</sup> on a four-layer broadband antireflection coating. The design is LMHHL QWOTS at  $0.51 \mu\text{m}$  with indices  $L = 1.38$ ,  $M = 1.47$ , and  $H = 2.09$ . The spectral reflectance is shown in Fig. 13, and the circle diagram for the design wavelength is shown in Fig. 14. It is clear from Fig. 14 that the turning points used to determine the optical thickness are at the ends of small

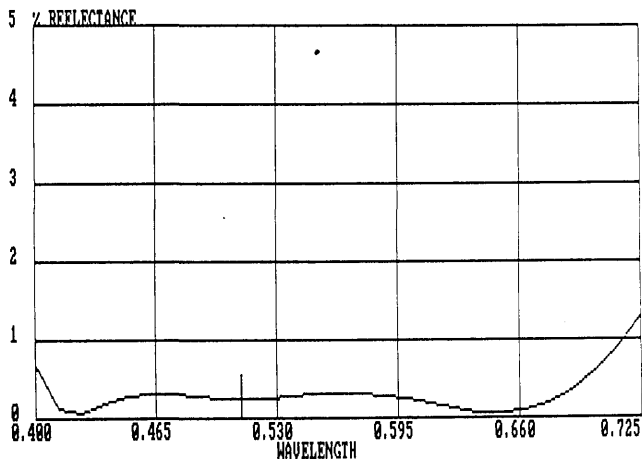


Fig. 13. Spectral reflectance of an antireflection coating of design LMHHL QWOTs after Ward,<sup>10</sup> which was analyzed by Macleod and Pelletier.<sup>1</sup>

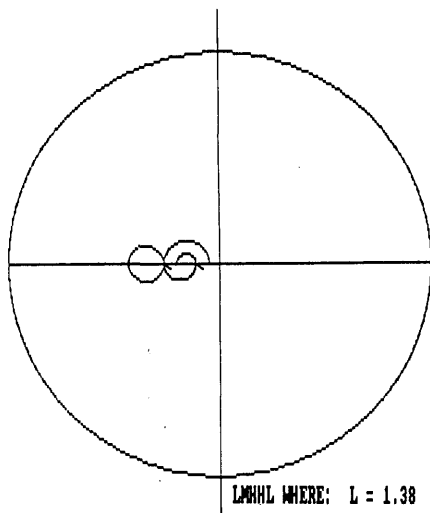


Fig. 14. Circle diagram of Ward's LMHHL antireflection coating without pre-coating.

circles in the region of the real axis, and large changes in optical thickness will cause only small changes in reflectance. The optical monitoring curve, Fig. 15, also emphasizes the small changes in reflectance with thickness. Macleod and Pelletier conclude that "...good results cannot be expected if there is no pre-coating..." and our observations agree.

The same authors concluded that "...one and two layers of pre-coating are fairly similar with a slightly better arrangement for two layers..." and that "Three and five layers... are rather poorer." Figures 16 and 17 show the circle diagram of the two-layer precoat and its monitor curve. It can be seen to enlarge the size of the circles 5 or 6 times, and the change of reflectance in monitoring is of the same order. However, the layer terminations are still at the least sensitive real axis position.

Figures 18 and 19 show the three-layer pre-coating case. The starting point for the four layers and the

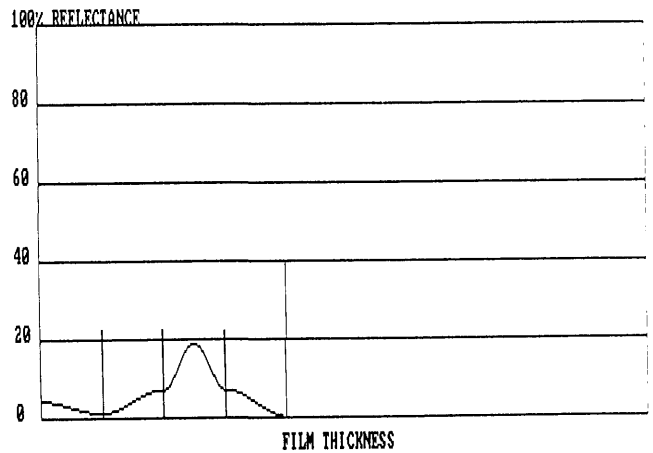


Fig. 15. Optical monitoring curve of Ward's LMHHL coating without pre-coating.

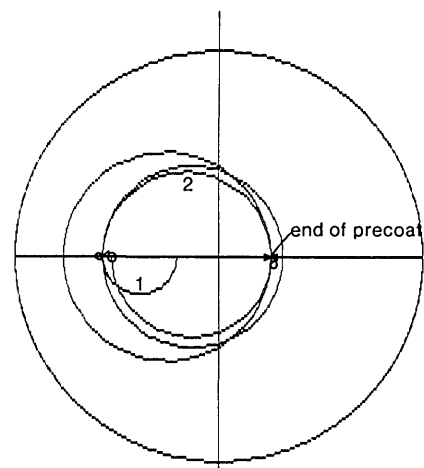


Fig. 16. Circle diagram of Ward's LMHHL coating with a two-layer pre-coating described by Macleod and Pelletier as the most satisfactory.

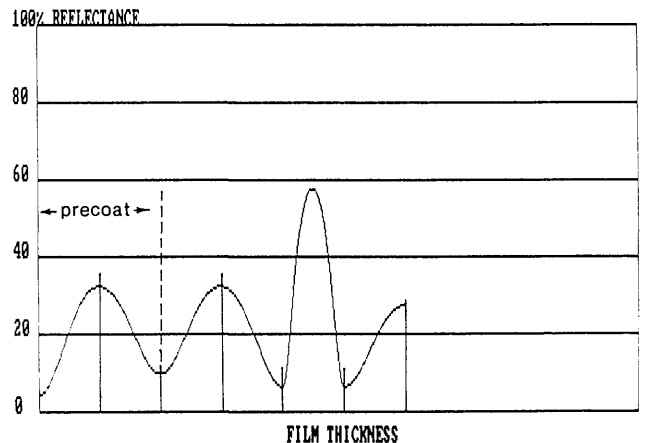


Fig. 17. Optical monitor curve of Ward's LMHHL coating with a two-layer precoat.

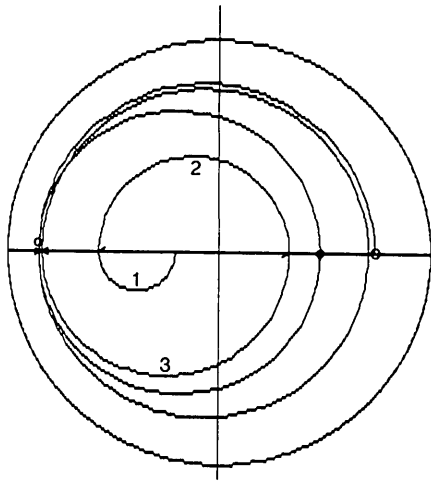


Fig. 18. Circle diagram of Ward's LMHHL coating with a three-layer precoat.

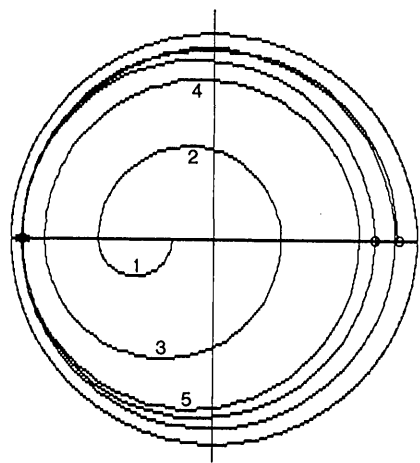


Fig. 20. Circle diagram of Ward's LMHHL coating with a five-layer precoat described by Macleod and Pelletier as the least satisfactory.

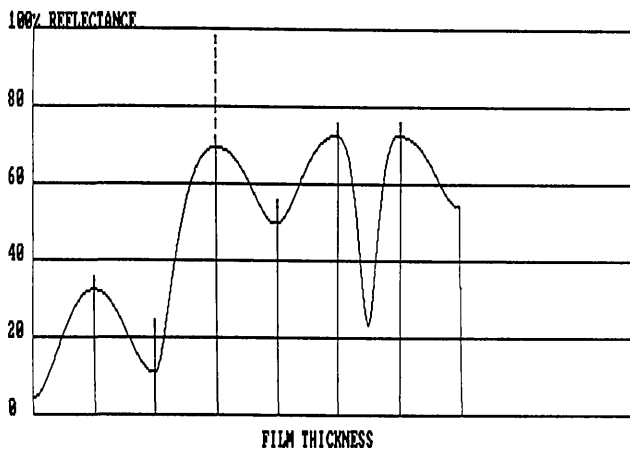


Fig. 19. Optical monitor curve of Ward's LMHHL coating with a three-layer precoat.

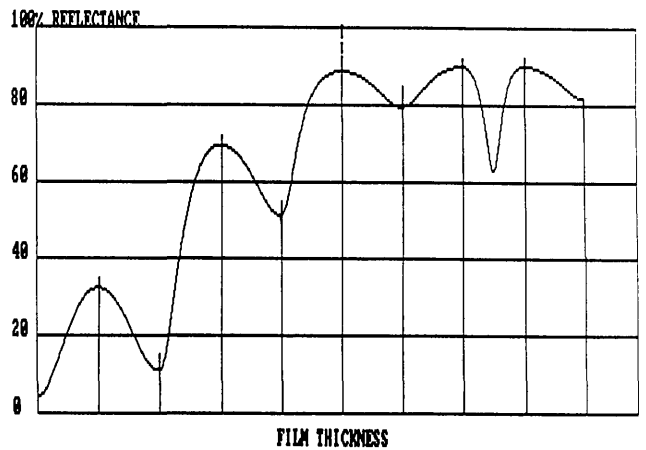


Fig. 21. Optical monitor curve of Ward's LMHHL coating with a five-layer precoat. Note that the layer terminations are compressed at the high-reflectance values.

termination of two of the layers are to be seen near the extreme left of the reflectance circle diagram where sensitivity approaches a minimum. It is not surprising, therefore, that this example helps us agree with the conclusions of Macleod and Pelletier.

Figures 20 and 21 show an extreme case with a five-layer precoat. Three of the terminations occur at the extreme of the real axis where sensitivity is at a minimum. Figure 21 illustrates that four layers of coating have monitor reflectance changes only a factor or 2 greater than the unprecoated case. Four layers are definitely inferior to the two-layer precoat strategy.

We investigated the possibilities of a nonquarter-wave single-layer precoat for this four-layer design using high-index material. Figure 22 shows our choice. We moved the termination points as far off-axis as practical with the high-index material. This occurs with either 1/8th or 3/8ths wave of high-index material and has the approximate effect of rotating the whole circle diagram clockwise by some amount and pushing the termination points away from the zero

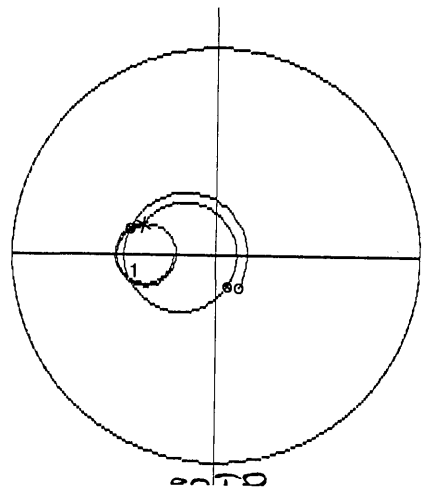


Fig. 22. Circle diagram of a single-layer nonquarterwave precoat for improved sensitivity in monitoring the Ward design.

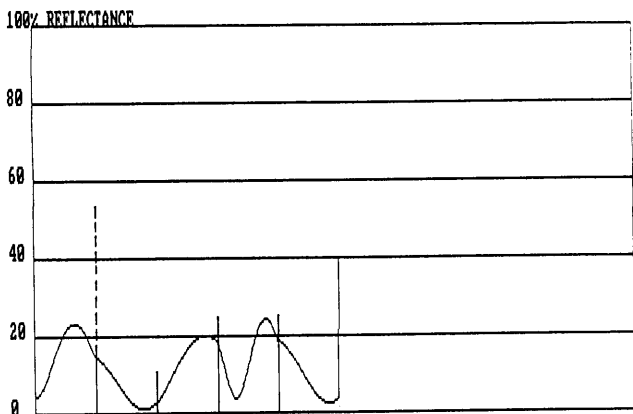


Fig. 23. Optical monitor curve of the optimized single-layer precoat for Ward's LMHHL design.

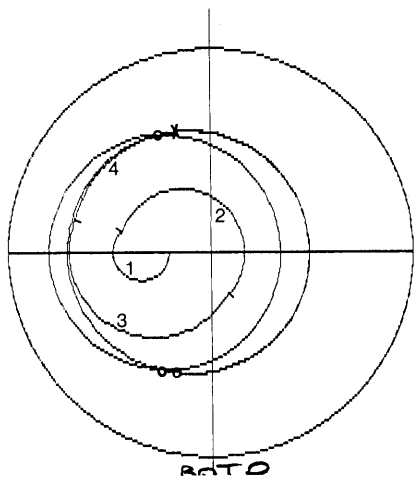


Fig. 24. Circle diagram of a four-layer precoat for the four-layer antireflection coating of Ward which maintains the termination points near the optimal sensitivity level.

sensitivity axis. The 3/8ths version is our preference because it makes the termination of the layers occur after an extremum of reflectance and can be used as a running calibration of the monitor.

The monitoring curve of Fig. 23 confirms the distinct advantages when compared with the two-layer precoat described above. This results because it terminates all the layers at points within 25–40% of the maximum sensitivity possible. A higher index single-layer precoat will improve the sensitivity up to an index of  $\sim 4$ , the optimum level point reached by a precoat.

If one is committed to precoating, it is almost as easy to deposit a multilayer precoat as a single layer. Since a chamber run must be dedicated to the precoat step, enough monitor chips can be made to cover many production runs of the coating for which the precoat is to be used. This helps minimize the process overhead. Therefore, we investigated working with an unlimited number of precoat layers. The best that we could hope for was to get all the layer termination points as near the maximum sensitivity point as possible. Although this can be further refined to in-

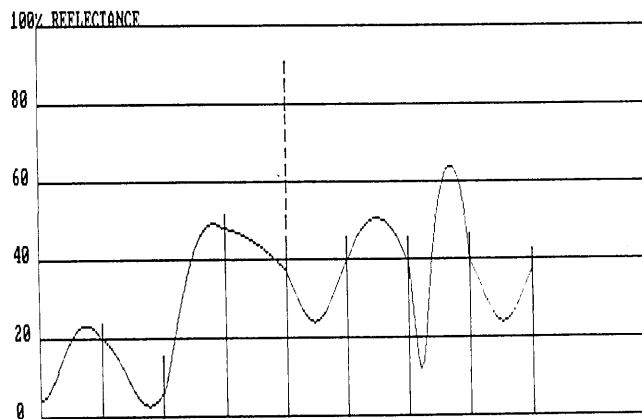


Fig. 25. Optical monitor curve of the optimum level precoat for the Ward LMHHL design.

clude sensitivity of the final coating to errors in the particular layers, that step is not part of this paper.

We chose to have the layers of the production coating terminate as near the maximum sensitivity point as the materials and monitoring wavelength allowed. We then designed the precoat to reach this desired starting point for the first layer. In most cases, we found that four layers of materials like magnesium fluoride and titanium dioxide are necessary to go from a crown glass substrate to the optimum level. Figure 24 shows such a four-layer precoat for the four-layer antireflection coating we have been discussing.

We chose to use what latitude was available in the precoat design to have its termination points also as close to the optimum level as practical. Figure 25 shows the resulting monitoring curve. This four-layer strategy is 3 times more sensitive than the optimum single-layer precoat strategy in this case.

## VI. Procedure

van der Laan<sup>11</sup> has recently described planning and procedures which he uses for optical monitoring of nonquarterwave stacks. His scheme utilizes a computer program for the planning. Our graphical procedure is illustrated with an example described recently by Zoller *et al.*<sup>12</sup> They converted a four-material broadband antireflection coating into a two-material equivalent of six layers. The approximate prescription in QWOTs is: 0.338H, 0.328L, 1.461H, 0.119L, 0.74H, 1.30L at a wavelength of  $0.54 \mu\text{m}$  with  $H = 2.08$  and  $L = 1.38$ . Figure 26 shows the spectral reflectance of the coating design, and Fig. 27 shows the circle diagram at the wavelength which they selected for semidirect monitoring.

They chose not to use precoat for improved monitoring accuracy to maintain "... flexible production in an optical coating shop." Figure 28 shows the monitoring curve they used to take some advantage of level terminations after turning points. In these circumstances they selected the wavelength which seemed to yield the best semidirect monitoring sensitivity. They compared the results of indirect and semidirect monitoring and concluded: "The single test slide monitor-

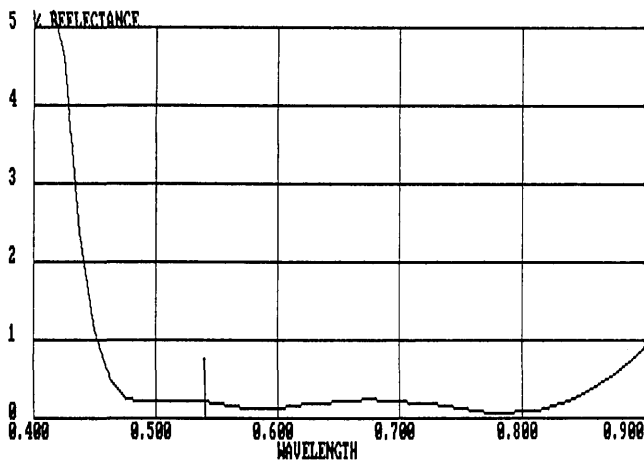


Fig. 26. Spectral reflectance of Zoller's<sup>12</sup> six-layer antireflection coating.

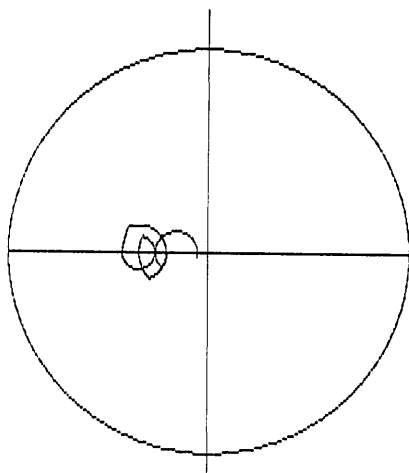


Fig. 27. Circle diagram of Zoller's six layers at the monitoring wavelength.

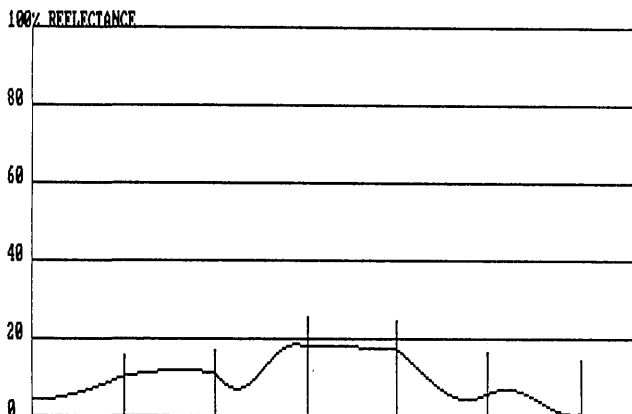


Fig. 28. Optical monitor curve used by Zoller *et al.* which takes advantage of level terminations after turning points.

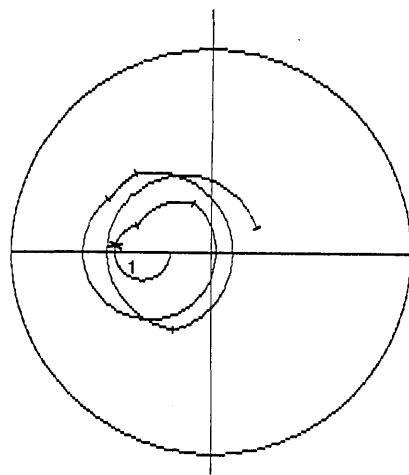


Fig. 29. Circle diagram of an optimized single-layer precoat for Zoller's design.

ing proved to yield a slightly better reproducibility due to better signal resolution and a small automatic error compensation effect."

We decided to see what could be accomplished by contrasting a single-layer with a multilayer precoat for this design. Our procedure for a single-layer precoat is the following:

(1) Construct a circle diagram for the coating starting with a quarterwave precoat of the highest-index material to be used for the application. Accentuate the terminal points of each layer on the diagram.

(2) Rotate the diagram clockwise and counterclockwise about the center of the high-index circle to see where the terminal points move the greatest distance from the real axis.

(3) Select an angle of rotation and use the amount of the single precoat which starts the first layer at that point.

(4) Reconstruct the diagram as in step (1) but with the new precoat. Make small adjustments in the precoat if the result is notably different from the prediction of step (2).

Figure 29 is the result of such a process, and Fig. 30 shows the monitoring curve to be compared with the unprecoated monitoring curve of Fig. 28.

The procedure for multilayer precoat is as follows:

(1) Start with the first layer of production coating at one of the optimum points and lay the layer thicknesses end to end clockwise around the circle diagram. Accentuate the termination points.

(2) Rotate the diagram about its general center to find where the terminal points are at the greatest distance from the real axis. Reconstruct step (1) after the desired rotation to correct for any changes resulting from rotation.

(3) Construct a precoat design which goes from the substrate to the start of the first layer and which has adequate sensitivity at the termination points of its layers. This will generally benefit by using overshoots as large as practical for cut point accuracy.

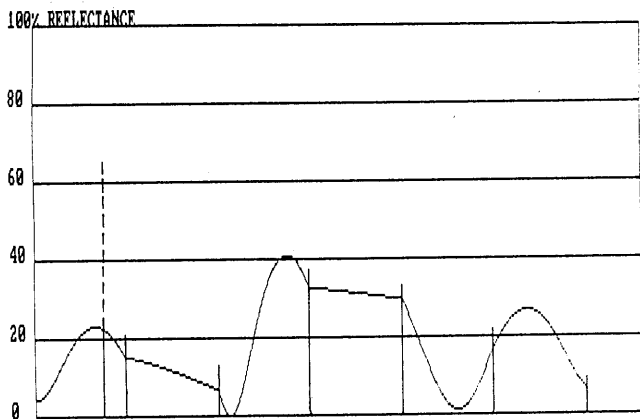


Fig. 30. Optical monitor curve for the optimized single-layer precoat for Zoller's design.

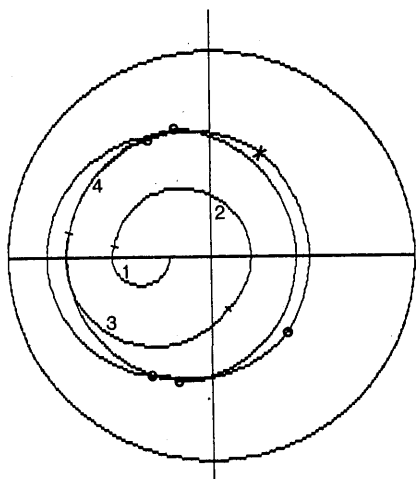


Fig. 31. Circle diagram of the application of the optimum sensitivity procedure to the design of a four-layer precoat for Zoller's six-layer antireflection coating.

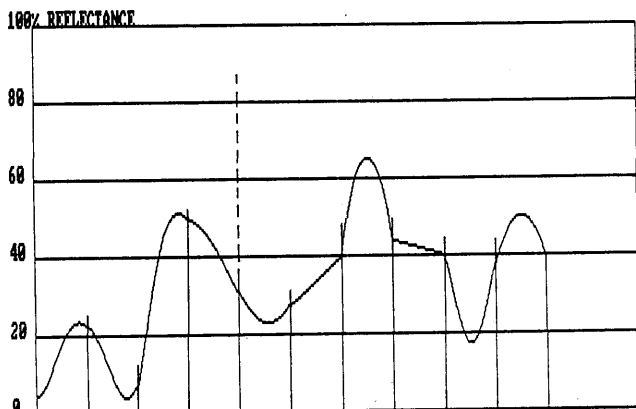


Fig. 32. Optical monitor curve of the four-layer precoat which has nearly optimum sensitivity levels for this coating design.

Figure 31 demonstrates the application of this procedure to the design of a four-layer precoat for Zoller's six-layer antireflection coating. Figure 32 shows the monitoring curve with nearly optimum sensitivity levels for the same coating design.

## VII. Conclusion

Utilizing the graphical aid of reflectance circle diagrams clarifies and refines procedures for semidirect optical monitoring of thin films. This has provided additional insight as to why various monitoring strategies differ in sensitivity.

Finally, introducing the concept of optimal semidirect level monitoring has yielded procedures useful for choosing more sensitive optical monitoring strategies. Since semidirect monitoring can give error compensation effects, and optimal level monitoring can reduce the magnitude of errors, the combination is expected to yield improved precision and repeatability in optical coating production.

## References

1. H. A. Macleod and E. Pelletier, "Error Compensation Mechanisms in Some Thin-Film Monitoring Systems," *Opt. Acta* **24**, 907 (1977).
2. F. Zhao, "Monitoring of Periodic Multilayer by the Level Method," *Appl. Opt.* **24**, 3339 (1985).
3. H. A. Macleod, "Monitoring of Optical Coatings," *Appl. Opt.* **20**, 82 (1981).
4. W. P. Thoni, "Deposition of Optical Coatings: Process Control and Automation," *Thin Solid Films* **88**, 385 (1982).
5. B. Vidal and E. Pelletier, "Nonquarterwave Multilayer Filters: Optical Monitoring with a Minicomputer Allowing Correction of Thickness Errors," *Appl. Opt.* **18**, 3857 (1979).
6. C. Schroedter, "Evaporation Monitoring System Featuring Software Trigger Points and On-Line Evaluation of Refractive Indices," *Proc. Soc. Photo-Opt. Instrum. Eng.* **652**, 15 (1986).
7. R. R. Willey, "Survey of Computer Numerically Controlled Optical Coating Systems," *Proc. Soc. Photo-Opt. Instrum. Eng.* **652**, 41 (1986).
8. J. H. Apfel, "Graphics in Optical Coating Design," *Appl. Opt.* **11**, 1303 (1972).
9. H. A. Macleod, *Thin-Film Optical Filters* (Macmillan, New York, 1986), pp. 61, 65.
10. J. Ward, *Vacuum* **22**, 369 (1972).
11. C. J. van der Laan, "Optical Monitoring of Nonquarterwave Stacks," *Appl. Opt.* **25**, 753 (1986).
12. A. Zoller, R. Herrmann, W. Klug, and W. Zültzke, "Optical Monitoring: Comparison of Different Monitoring Strategies with Respect to the Resulting Reproducibility to the Completed Layer Systems," *Proc. Soc. Photo-Opt. Instrum. Eng.* **652**, 21 (1986).